Improved strain based finite element for the elasto-plastic analysis

Djouama Mohamed Lamine [1,a]*, Djamal Hamadi[2,b], Abdelhak Khechai[3,c]

[1, 2] Laboratory of Civil Engineering, Hydraulics, Development and Durability, Department of Civil Engineering and Hydraulics, Biskra University, B.P. 145 RP, 07000 Biskra, Algeria

[3] Laboratory of Civil Engineering, University of Biskra, Biskra 07000, Algeria

[a,]Emails: m.djouama@univ-biskra.dz , [b]Emails: d.hamadi@univ-biskra.dz,*

[c]Email: abdelhak_khechai@hotmail.fr

**E-mail address of the corresponding author: m.djouama@univ-biskra.dz (M.L. Djouama)*

Abstract

In the present paper, a finite element on the strain-based approach is developed to foresee the behavior of a nonlinear isotropic materials, The displacement fields of the present membrane element is the same as adopted by Sabir [1] and the supposed functions for components of strains are satisfy the compatibility equations. This element has four nodes and two degrees of freedom in each node as previously developed by Sabir et al.[1] for linear analysis. In this paper, this element is extended to predict accurately the elasto-plastic behavior of two-dimensional problems. In order to analyze the elasto-plastic comportment, several yield criterions are employed such as von-Mises, Mohr-Coulomb, Tresca and Drucker-Prager. In this study, the method of the tangential stiffness is adopted to recalculating the element stiffness matrix for each iteration. Through the numerical applications, the results given by the current element for the linear and nonlinear analysis are compared with those available in the literature. It is observed that the results obtained are very near to the results of the reference and this demonstrated the efficiency of the formulated element. By using the same number of nodes, the numerical solutions based on the strain-based approximation has higher precision than the element based on classical displacement approach. Finally, to appear the impact of a few parameters on elasto-plastic response, a number of applications for different strain hardening values are given and discussed. Very interesting comments and conclusions are pointed out for the efficiency of the strain based approach for the elasto-plastic analysis.

***Keywords*:** *Stain-based approach, linear analysis, elasto-plastic analysis, strain hardening parameter, yield criterion.*

Introduction

For many years, researchers have proposed different finite element models based on various approaches to predict the linear [2, 3] and nonlinear behavior of some structural components [4] One of these methods is the strain-based approach. The positive features of this approach have been illustrated on several studies[5, 6] compared to the displacement approach [7]. The development of finite elements based on the strain approach has initially been formulated by Sabir [1] and the displacement fields are obtained by the strain integration. In the literature, the utilize of the strain-based approach for the improvement of a new family of finite elements was first applied by Ashwell and Sabir [8] for general plane elasticity problems. In their work, Ashwell and Sabir[9] developed a finite element to analyze curved structural. Several finite elements were also developed by Sabir [10]], notably SBRIE, (Strain-Based Rectangular In-plane Element), the rectangular finite element based on a constant shearing strain and linear variation of the direct strains.

Later, Several versions of the SBRIE were suggested by Sabir et al. [1] and used under the names (SBRIE1), and (SBRIE2) in order to analyze general plane elasticity problems. On the other hand, the strain-based approach was also enlarged to the development of new simple and efficient triangular and rectangular elements having an in-plane rotation (drilling rotation) as a one of the nodal degrees of freedom[11] for both two-dimensional and three-dimensional elasticity problems[12]] proposed a new finite triangular element for the static bending analysis and the free vibration of plates. The proposed element contains three exterior degrees of freedom in each node based on Reissner/Mindlin theory. The strain-based approach was also applied to investigate the behavior of the geometrical nonlinear of the circular arches [13] and the large deflection of shells[14] In his work, Sabir et al.[14] focused on analyzing only the large deflection and the behavior of geometrical nonlinear shells and complex load-deflection curves were given for cylindrical and spherical shells by increasing loads as well as deflections. Recent researches have also given more importance to the problem of the nonlinear behavior of isotropic materials. Rebiai et al.[15-17] developed a quadrilateral membrane element and a triangular finite element, having an in-plane rotation as a nodal degree of freedom, for both elasto-viscoplastic and dynamic analysis respectively.[18] improved an eight-node quadrilateral membrane finite element element denoted PFR8 (Plane Fiber Rotation) with rotational degrees of freedom, for elasto-plastic analysis. [19] implemented in ABAQUS an existing robust three dimensional finite element based on the strain approach for the static and dynamic analysis of isotropic plates. More recently,[20] developed a new four node rectangular finite element for bending analysis of thin plates, for linear analysis. In same way, [21] developed a pentagonal membrane element with the strain based approach, a pentagonal mesh was created, and the mesh quality was improved with Laplacian smoothing. However, in the open literature and based on the strain approach, there is not a deep analysis on the Elasto-plastic behavior. Based on the displacement approach, the literature showed that the quadrilateral membrane element with four nodes Q4 can be quite stiff in certain deformation modes, whereas the quadrilateral membrane element with eight nodes Q8 can be computationally expensive, involving as it does 16 degrees of freedom.

In this paper, a rectangular finite element, previously developed by Sabir et al. [1] for the linear analysis is extended to predict accurately the elastoplastic analysis of two-dimensional problems. In order to distinguish between the SBRIE and the present element, the extended element is named SBRIEPE (Strain Based Rectangular In-plane Elasto-Plastic Element), with four corner nodes and in each node has two degrees of freedom (two translations). For the elasto-plastic analysis, several yield criterions are employed such as von-Mises, Drucker-Prager, Mohr-Coulomb and Tresca criteria. The tangential stiffness method is adopted.

First, in this paper a description of the SBRIE finite element formulation is given and a review of some yield criterions for analyzing the elasto-plastic behavior of isotropic materials are defined. To make clear the efficiency and the performance of SBRIEPE, some validation tested are presented for the linear analysis. Then, for the main objective of this work, the two-dimensional elastoplastic analysis is carried out through with applications. It is should be mention that, the numerical results given by the present element for both linear and nonlinear analysis are compared with those found in the literature. It is observed that the obtained results are very close to the reference results which illustrates the good accuracy and efficiency of the present element for the elasto-plastic behavior.

1.Mathematical Formulation of the SBRIE Element.

The rectangular strain-based finite element **SBRIE** [1] with two degrees of freedom per node (u_i and v_i) is shown in Fig. 1. With a and b are the length sides in both directions x and y, respectively.

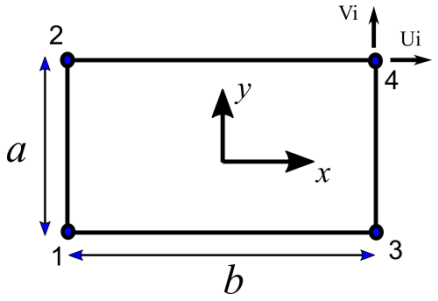

Fig. 1. Geometry and coordinate system of the element **SBRIE**

The displacement field should include eight independent constants. The three strain components at any point in the element can be expressed in terms of displacements as

$$\varepsilon_x = \frac{\partial u}{\partial x},\ \varepsilon_y = \frac{\partial v}{\partial y},\ \gamma_{xy} = \frac{\partial u}{\partial y} + \frac{\partial v}{\partial x} \tag{1}$$

In the case where the strain equations given by eq. (1) equal to zero, the integration of the strains gives the displacement field in terms of the three rigid body displacements at presented in the following expression

$$\begin{aligned} u &= \alpha_1 - \alpha_3 y \\ v &= \alpha_2 + \alpha_3 x \end{aligned} \tag{2}$$

Equation (2) gives the two components of rigid body displacements. The equation (1) of the strains is not independent since they are in relation with the displacements u and v.

Hence, it is essential that strains must satisfy the compatibility equation, which obtained by eliminating *u* and *v* form equation (1), hence

$$\frac{\partial^2 \varepsilon_x}{\partial y^2}+\frac{\partial^2 \varepsilon_y}{\partial x^2}-\frac{\partial^2 \gamma_{xy}}{\partial x \partial y}=0 \tag{3}$$

The SBRIE has four nodes and two degrees of freedom per node (*u*, *v*). Hence the independent constants must be eight, three of three of displacements of rigid body $(\alpha_1,\alpha_2,\alpha_3)$ given by eq. (2) and five other constants $(\alpha_4,\alpha_5.....,\alpha_8)$ have to be added for expressing the displacement. The five constants among the strain are presented as follow [1]:

$$\begin{aligned}\varepsilon_x &= \alpha_4+\alpha_5 y\\ \varepsilon_y &= \alpha_6+\alpha_7 x\\ \gamma_{xy} &= \alpha_8\end{aligned} \tag{4}$$

It should be mentioned that the strains of equation (4) satisfy the compatibility equation (3) and after the integration and substitution into Eq. (2), the final displacement functions are given as follow:

$$\begin{aligned}u &= \alpha_1-\alpha_3 y+\alpha_4 x+\alpha_5 xy-\alpha_7 y^2/2+\alpha_8 y/2\\ v &= \alpha_2+\alpha_3 x-\alpha_5 x^2/2+\alpha_6 y+\alpha_7 xy+\alpha_8 x/2\end{aligned} \tag{5}$$

Equation (4) can be rewritten in matrix form as $\{\varepsilon\}=[Q]\{\alpha\}$ where the matrix $[Q]$ relating the strain fields to the unknown constants $\{\alpha\}$ and is given by:

$$[Q]=\begin{bmatrix}0&0&0&1&y&0&0&0\\0&0&0&0&0&1&x&0\\0&0&0&0&0&0&0&1\end{bmatrix} \tag{6}$$

And the displacement functions given by eq. (5) and can also be written in a matrix form as[1]:

$$\{U\}=[C]\{\alpha\} \tag{7}$$

Where $\{U\}$ is the displacement vector, and $[C]$ is the nodal coordinates matrix and is given in the appendix.

The element stiffness matrix $[K_e]$ can be obtained using the well-known expression

$$[K_e]=\int_V [B]^T [D][B]dV \tag{8}$$

Where $[D]$ is the matrix of elasticity, and $[B]$ is the stain-displacement matrix is given as follow

$$[B]=[L]\{U\}.[C^{-1}]=[Q][C^{-1}] \tag{9}$$

$$[L]=\begin{bmatrix} \frac{\partial}{\partial x} & 0 \\ 0 & \frac{\partial}{\partial y} \\ \frac{\partial}{\partial y} & \frac{\partial}{\partial x} \end{bmatrix}$$

Where $[L]$ is the differential operator matrix.

The element stiffness matrix $[K_e]$, for a unit thickness becomes

$$[K_e]=\left[C^{-1}\right]^T\left[\iint_s [Q]^T[D][Q]dx.dy\right]\left[C^{-1}\right]=\left[C^{-1}\right]^T[K_0]\left[C^{-1}\right] \quad (10)$$

The elasticity matrices for both plane stress and plane strain problems are given in the appendix.

2. Formulation of the Tangential Stiffens Matrix $[K_T]$ for Elasto-plastic Behavior

To determine the beginning point of the plastic phase, it is necessary to define the yield function that can be written as [22, 23]

$$f(\sigma)=Y(k) \quad (11)$$

Or $F(\sigma,k)=f(\sigma)-Y(k)=0$ (12)

Where the function of stress is f, Y is the function of hardening parameter, σ is the stress vector, k is the hardening parameter, which governs the expansion of the yield surface. By differentiating eq. (12) one can get

$$dF=\frac{\partial F}{\partial \sigma}d\sigma+\frac{\partial F}{\partial k}dk=0 \quad (13)$$

Or $a^T d\sigma - A d\lambda = 0$ (14)

where: $a^T=\frac{\partial F}{\partial \sigma}$ (15)

and $A=-\frac{1}{d\lambda}\frac{\partial F}{\partial k}dk$ (16)

The vector *a* is the flow vector, the incremental relationship between stress and strain of elasto-plastic deformation could be written as

$$d\varepsilon=[D]^{-1}d\sigma+d\lambda\frac{\partial F}{\partial \sigma} \quad (17)$$

With $[D]$ the elastic matrix. pre-multiplying both sides of eq. (16) by $d_{DT}=a^T D$ and eliminating $a^T d\sigma$ by use of Eq. (14) one can obtain the plastic multiplier $d\lambda$

$$d\lambda=\frac{1}{\left[A+a^T Da\right]}a^T d_D d\varepsilon \quad (18)$$

Substituting Eq. (18) into Eq. (17) could be given the stress-strain incremental elasto-plastic relation

$$d\sigma = D_{ep} d\varepsilon \tag{19}$$

With D_{ep} is the elasto-plastic matrix

$$D_{ep} = D - \frac{d_D \, d_{D^T}}{A + d^T a}, \quad d_D = Da. \tag{20}$$

The work hardening hypothesis is more general from a thermodynamic viewpoint than the strain-hardening assumption and will be employed for numerical work in this text. Therefore

$$dk = \sigma^T d\varepsilon_p \tag{21}$$

And Eq. (12) can be rewritten in the form

$$F(\sigma, k) = f(\sigma) - \sigma_Y(k) = 0 \tag{22}$$

Since the uniaxial yield stress, $\sigma_Y = \sqrt{3}k$. Thus from Eq. (16)

$$A = -\frac{1}{d\lambda}\frac{\partial F}{\partial k} dk = \frac{1}{d\lambda}\frac{\partial \sigma_Y}{\partial k} dk \tag{23}$$

Noting that the full differential may be employed in the last term since σ_Y is a function of *k* only. Employing the normality condition in Eq. (21) to express $d\varepsilon_p$ one can get

$$dk = \sigma^T d\varepsilon_p = \sigma^T d\lambda a = d\lambda a^T \sigma \tag{24}$$

Or, for the uniaxial case $\sigma = \bar{\sigma} = \sigma_Y$ and $d\varepsilon_p = d\bar{\varepsilon}_p$ where $\bar{\sigma}$ and $\bar{\varepsilon}_p$ are respectively the effective stress and strain. Thus Eq. (24) becomes

$$dk = \sigma_Y d\bar{\varepsilon}_p = d\lambda a^T \sigma \tag{25}$$

and

$$\frac{d\bar{\sigma}}{d\bar{\varepsilon}_p} = \frac{d\sigma_Y}{d\bar{\varepsilon}_p} = E' \tag{26}$$

For the elastoplastic solution can use the principle of virtual work, which requires that:

$$\int_\Omega \left(\delta\varepsilon^{*T}\sigma - \delta u^{*T} b\right) d\Omega - \delta d^{*T} f = 0 \tag{27}$$

With σ is the internal stresses, *b* is the distributed loads/unit volume and f is external applied forces form an equilibrating field. δd^* is the arbitrary virtual displacement, $\delta\varepsilon^*$ is the compatible strain, and δu^* is the internal displacements.

$$\delta u^* = N\delta d^*, \quad \delta\varepsilon^* = B\delta d^* \tag{28}$$

With *N* is the function shape matrix and *B* is the elastic strain matrix, where substituting Eq. (28) into Eq. (27) one can obtain

$$\int_\Omega \delta d^{*T} \left(B^T\sigma - N^T b\right) d\Omega - \delta d^{*T} f = 0 \tag{29}$$

Or

$$\int_\Omega B^T \sigma d\Omega - f - \int_\Omega N^T b d\Omega = 0 \tag{30}$$

For the solution of nonlinear problems Eq. (30) will not be satisfied at any stage of the calculation in the nonlinear analysis

$$\psi = \int_{\Omega} B^T \sigma d\Omega - f - \int_{\Omega} N^T b \, d\Omega \neq 0 \tag{31}$$

where ψ is the vector of residual force. In the elasto-plastic analysis, the strain/stress equation given by Eq. (19) and the material stiffness is continually varying. It must be added to the Eq. (31) for the calculation of the tangential stiffness matrix $[K_T]$ for any stage. Hence, at any increment of load we have:

$$\Delta\psi = \int_{\Omega} B^T \Delta\sigma \, d\Omega - \left(\Delta f + \int_{\Omega} N^T \Delta b \, d\Omega \right) \tag{32}$$

Substituting for $\Delta\sigma$ from Eq. (19) gives

$$\Delta\psi = K_T d - \left(\Delta f + \int_{\Omega} N^T \Delta b \, d\Omega \right) \tag{33}$$

where

$$K_T = \int_{\Omega} B^T D_{ep} B d\Omega \tag{34}$$

2.2 The Tangential Stiffness Solution Method

In the nonlinear analysis, the stiffness matrix $[K_e]$ of a linear analysis becomes a tangential matrix $[K_T]$. The analysis must be proceeding in an incremental manner and the problem can be linearized over any increment of load. For this reason, the numerical solution processes for nonlinear problems named the tangential stiffness method. The solution is started from a trial value of displacement u^0, and the tangential stiffness matrix $[K_T](u^0)$ corresponding to this displacement will be determined as well as the residual force ψ^0. The solution algorithm for this method given as follow:

$$\Delta u^r = -\left[K_T \left(u^r \right) \right]^{-1} . \psi \left(u^r \right) \tag{35}$$

An improved approximation of the displacement is then obtained as $u^1 = u^0 + \Delta u^0$. The iteration continued until the convergence achieved.

3.The Yield Criterion: A yield criterion is the elasticity limit and the start of plastic deformation. The yield criterion utilized in the present study are Tresca criteria, von Mises criteria, Mohr-coulomb criteria, Drucker-Prager criteria [22].

3.1 Tresca criteria: Tresca proposed that yielding begins when the extreme shear stress comes a certain value. The expression of the Tresca criteria is given as following

$$F = 2\bar{\sigma} \cos\phi - Y(k) = 0 \tag{36}$$

Where

$$\bar{\sigma} = \left[\frac{1}{2} \left(s^2{}_x + s^2{}_y + s^2{}_z \right) + \tau^2{}_{xy} + \tau^2{}_{yz} + \tau^2{}_{zx} \right]^{1/2}$$

$$s_x = \sigma_x - \sigma_m, \; s_y = \sigma_y - \sigma_m, \; s_z = \sigma_z - \sigma_m$$

$$\sigma_m = \frac{1}{3}(\sigma_x + \sigma_y + \sigma_z)$$

$$\phi = \frac{1}{3}\sin^{-1}\left[-\frac{3\sqrt{3}}{2}\frac{J_3}{\bar{\sigma}^3}\right], \text{ with } -1/6\pi \le \phi \le 1/6\pi$$

$$J_3 = s_x s_y s_z + 2\tau_{xy}\tau_{yz}\tau_{xz} - s_x\tau^2_{yz} - s_y\tau^2_{xz} - s_z\tau^2_{xy}$$

$Y(k)$ is the yield stress obtained from a uniaxial test

3.2 Von-Mises Criteria: Von-Mises suggested that yielding occurs when $J_2' = \bar{\sigma}$ comes a critical value. The von-Mises criteria expression is given as following

$$F = \sqrt{3}\bar{\sigma} - Y(k) = 0 \quad (37)$$

3.3 Mohr-Coulomb Criteria: Mohr-Coulomb suggested that the complete yield surface is obtained by considering all other stress combinations, which can cause yielding. The expression of Mohr-Coulomb criteria is given as following

$$F = \sigma_m \sin\theta + \bar{\sigma}\cos\phi - \bar{\sigma}/\sqrt{3}\sin\phi\sin\theta - c\cos\theta = 0 \quad (38)$$

Where $c(k)$ and $\theta(k)$ are the cohesion and angle of friction, respectively, which could depend on some strain hardening parameter *k*.

3.4 Drucker-Prager Criteria: Drucker and Prager suggested that the effect of the component of hydrostatic stress on yielding was introduced by the inclusion of a supplemental term in the Von-Mises expression to get

$$F = 3\alpha'\sigma_m + \bar{\sigma} - k = 0 \quad (39)$$

where

$$\alpha' = \frac{2\sin\theta}{\sqrt{3}(3-\sin\theta)} \ , \ k = \frac{6\cos\theta}{\sqrt{3}(3-\sin\theta)}$$

4. Validation of SBRIE in the Linear Analysis

In this section, two examples for plane elasticity problems are tested. These test problems can be considered as a numerical validation of the level of accuracy obtained using SBRIE element. The obtained results are compared with different theoretical references and other finite elements available in the literature.

4.1 Allman's Cantilever Beam

In this test problem, the free end of the short cantilever beam is subjected to a vertical load with resultant *W*=40 K (see Fig. 2). The dimensions of the cantilever beam are the length *L*= 48 in, the width *H*=12 in and the thickness *t* = 1 in. The material properties are the Young's modulus *E*= 3.10^4 Ksi and the Poisson's ratio *v* = 0.25. This example test is usually considered by many researchers as a benchmark test to validate the efficiency of the developed plane elements. The results of the maximum displacements at the free edge of the beam are given in Table 1.

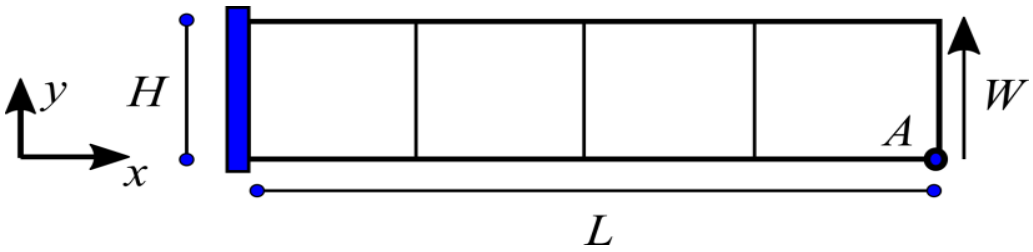

Fig. 2. Allman's cantilever beam data and mesh

Table 1. Normalized deflection for Allman's short cantilever beam subjected to a vertical load

Elements	Allman [24]	Q4	Q8 [25]	AQ [26]	MAQ [27]	SBRIE
Normalized vertical displacement at point A	0.852	0.679	0.985	0.918	0.918	0.928
Reference solution [28]	**1.000 (0.3553)**					

The results of the maximum deflection at the free end presented in Table 1 show that the accuracy of the **SBRIE** element is very good compared to the reference solution is slightly lower than the robust element Q8 (with 8 nodes).

4.2Mac-Neal's Elongated Cantilever Beam

In the second test, the cantilever beam as presented in Fig.3 is subjected to a concentrated shearing load at the free edge of the beam (P=1) and to a pure bending moment (M=10). This test is known in the literature as a Mac-Neal's beam [29]. The Length and the width of the beam respectively are L=6 and H=0.2. and the Young's modulus E=10^7, the Poisson's ratio v=0.3, and a thickness t is equal to 0.1. The numerical results of the normalized deflection for both loading cases are given in Tables 2 and 3.

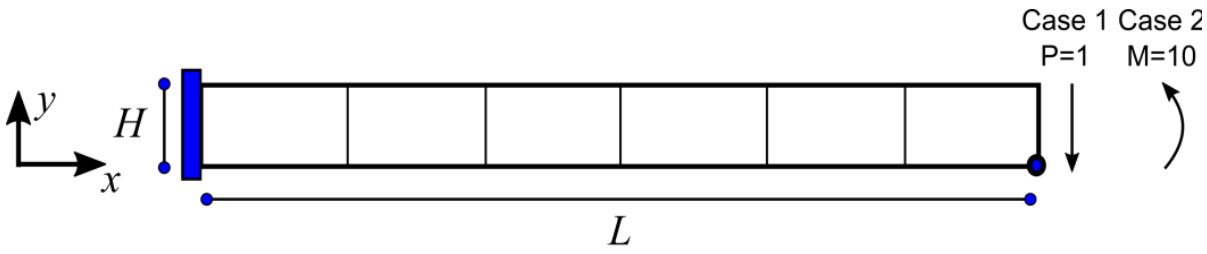

Fig. 3. Mac-Neal's elongated cantilever beam data and mesh

Table 2. Normalized maximum deflection for Mac-Neal's beam under pure bending

Elements	Q8 [25]	AQ [26]	MAQ [27]	Q4	SBRIE
Normalized vertical displacement at A	0.987	0.904	0.904	0.093	0.903
Reference solution	**1.000 (0.1081)**				
AQ = four node, 12 degree of freedom Allman-type quadrilateral obtained from Q8 MAQ = Mixed AQ.					

Table 3. Normalized maximum deflection for Mac-Neal's beam under shear loading.

Elements	Q8 [25]	AQ [26]	MAQ [27]	Q4	SBRIE
Normalized vertical displacement at A	0.991	0.910	0.910	0.093	0.910
Reference solution	**1.000 (0.270)**				

One can see from both tables that the SBRIE element gives the same results compared to AQ [26] and MAQ [27] and it is relatively in good agreement with the Q8. On the other hand, the element has achieved a very acceptable convergence to the reference solution in both cases under consideration (the shearing and a pure bending loading).

5.Validation of The Developed SBRIEPE in Elasto-plastic Behavior

In the current structural theories, one can observe an increasing interest in the computational approaches to analyze the elasto-plastic behavior. The analysis of elasto-plastic accounts for the nonlinear comportment of the material. During the work loading stage, and after surpassing the yield strength, the material's stiffness is different from that in the elastic phase. Accordingly, the complex of analysis of the present problem create a great challenge for researchers.

To overcome this difficulty, numerous studies attempted to develop new numerical techniques for elasto-plastic analysis. In this work, extended the **SBRIE**, previously developed by Sabir et al. [1] for the linear analysis, to predict accurately the elastoplastic analysis of two-dimensional problems. Several yield criterions are considered such as von-Mises, Tresca, Drucker-Prager, Mohr-Coulomb criterion.

In this investigation, two different tests are considered to validate the capability and the performance of the extended element **SBRIEPE**. The results are compared to some numerical solutions and to the other methods.

5.1 A Cantilever Beam Subjected to a Distributed Loading

In this test, a cantilever beam subjected to a distributed load is studied as shown in Fig. 4. The dimensions of the beam are chosen to be the length L=8 m and the height H=1 m and a unite thickness of the beam is considered and is treated as a plane stress problem. The beam is subjected to a distributed loading q = 1 N/m. The material properties used in the present analysis are the Young's modulus E= 10^5 Pa, the Poisson's ratio ν = 0.25, the yield strength σ_s = 25 Pa and the strain hardening parameter E'= 0.2 E and the Von-Mises yield criterion is used in this experiment. This problem has been also treated by Miaojuan et al. [30] using the

Complex Variable Element-Free Galerkin (CVEFG) method. The beam is divided into 10 and 4 elements in *x* and *y* directions, respectively.

The numerical results of the vertical displacements obtained with **SBRIEPE** element, ANSYS© and CVEFG method are presented in Table 4. It can be seen that the results obtained with **SBRIEPE** are in very acceptable. The small differences of the present results compared with the reference findings (ANSYS© results) can be related to the difference between the different approaches used from one hand, and to the numerical methods used for solving the problem (number of Gauss points in CVEFG method is 3x3), from another hand.

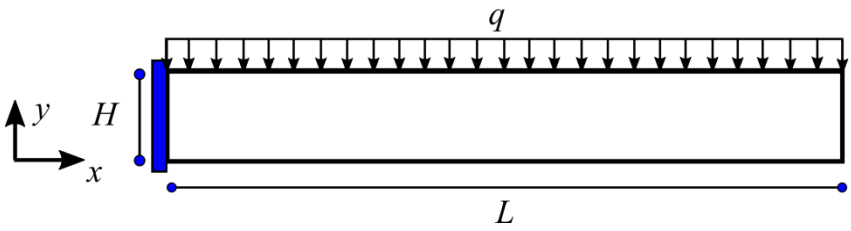

Fig.4. The geometry of a cantilever beam subjected to a distributed loading

Table 4. Nodal displacements of the cantilever beam subjected to a distributed load

Node Coordinate	**(1.6,0.5)**	**(3.2,0.5)**	**(4.8,0.5)**	**(6.4,0.5)**	**(8.0,0.5)**
ANSYS [30]	18.279	60.587	113.120	167.960	223.190
CVEFG [30]	18.554	60.310	111.814	166.413	221.317
Present SBRIEPE	14.880	51.910	98.554	147.504	196.877

5.2 A Cantilever Beam Subjected to a Concentrated Loading

In the second experiment test, a cantilever beam subjected to a concentrated load is studied, as shown in Fig. 5. The dimensions of the beam are chosen to be length L= 8 m, the height H = 1 m and the depth of the beam t = 1 m. This test has been also treated as a plane stress problem. The beam is subjected to a concentrated force at the free end of the beam. The concentrated applied load P = 1 N. The material properties used in the present analysis are the Young's modulus E= 10^5 Pa, the Poisson's ratio ν = 0.25, the yield strength σ_s = 25 Pa, and the strain hardening parameter is E'=0.2E and von-Mises yield criterion is adopted in this example. This problem has been also treated by Miaojuan et al. [30] using the CVEFG and the Element-Free Galerkin (EFG) method. The beam is divided into 10 and 4 elements in *x* and *y* directions, respectively. The numerical results of the vertical displacements obtained with **SBRIEPE** element are compared to those obtained with ANSYS©, CVEFG and EFG methods and are presented in Table 5.

Fig.5. The geometry of a cantilever beam subjected to a concentrated force

The results found with SBRIEPE element are compared to those obtained with ANSYS© software, CVEFG and EFG methods. It can be concluded that the results of SBRIEPE element are very acceptable.

Table 5. Nodal displacements of the cantilever beam subjected to a distributed loading

Node coordinate	**(1.6,0.5)**	**(3.2,0.5)**	**(4.8,0.5)**	**(6.4,0.5)**	**(8.0,0.5)**
ANSYS [30]	2.020	6.837	13.227	20.600	28.460
EFG [30]	1.946	6.728	13.077	20.409	28.236
CVEFG [30]	2.068	6.904	13.303	20.666	28.524
SBRIEPE	1.853	6.573	12.899	20.204	27.994

6. Parametric Study:

In this section, a parametric study will be present in the aim to determine the effect of some parameters, such as the strain hardening parameter on the nonlinear behavior of two-dimensional problems. Several yield criterions are considered such as the Von-Mises, Tresca, Mohr-Coulomb and Drucker-Prager criterion.

6.1 Short Cantilever Beam of Allman

In this problem, the free end of the short cantilever beam is subjected to vertical load, which increases incrementally (Fig. 2). The yield stress of the considered material is σ_s= 235 ksi. The strain hardening parameter are E'= 0 and E'= 0.2E. This test has been treated as a plane stress problem. The relationship between the displacements and the resulting stress is shown in Fig. 5. On can see from the figure that during the loading stage and after exceeding the elastic limit, the material begins yielding and enters into the plastic regime. Fig. 5 shows also the effect of the strain hardening parameter using different yielding criterion. One can see from the figure that by increasing the strain hardening value the stress increases. Both Tresca and von-Mises yielding criterion have the almost the same behavior. The same observation can be noticed for Mohr-Coulomb and Drucker-Prager criterion.

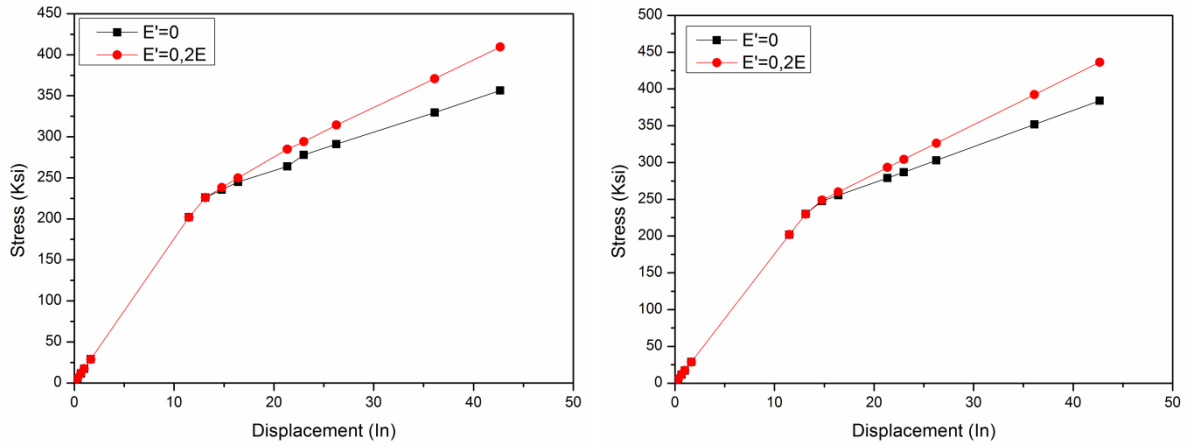

(a) Tresca criteria (b) von-Mises criteria

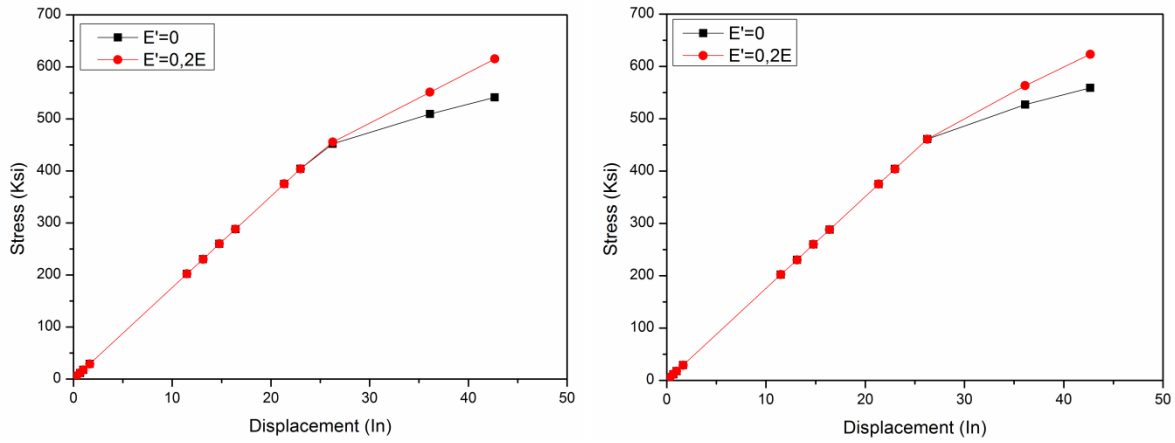

(c) Mohr-Coulomb criteria (d) Drucker-Prager criteria

Fig.5. Stress/displacement curves of Allman's cantilever beam using different values of strain hardening and various yielding criterion

6.2 Plane Flexure of Cantilever Beam

In the second problem, the free end of the cantilever beam is subjected to a vertical load (Fig. 6). The load is applied at the free edge of the beam incrementally. The dimensions of the cantilever beam are: the length L= 100, the width H=10 and the thickness t =1. The material properties are the Young's modulus E= 10^7, the Poisson's ratio v = 0.25 and the yield stress σ_s = 235. The strain hardening parameter is chosen to be E'= 0 and E'=0.2E. The relationship between the displacements and the resulting stress is presented in Fig. 5. It can be seen from the figure that during the loading stage and after exceeding the elastic limit, the material begins yielding and enters into the plastic regime. Figure 5 shows also the strain hardening parameter effect with different yielding criterion. Also, by increasing the strain hardening value the stress increases. The Tresca and Von-Mises yielding criterion have almost the same behavior. Finally, the same observation for Drucker-Prager and Mohr-Coulomb criterion can be noticed.

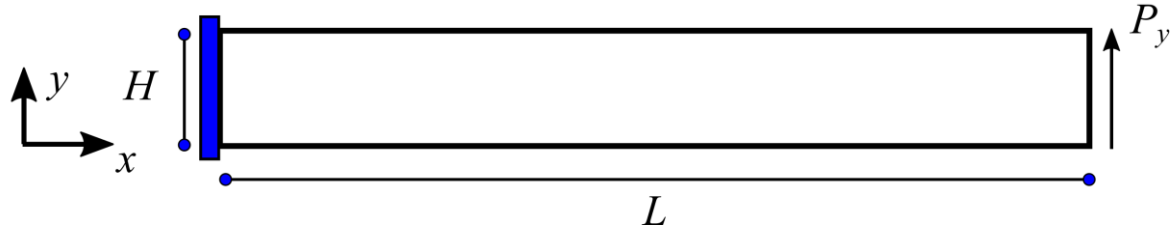

Fig 6. The geometry of a cantilever beam subjected to a concentrated load

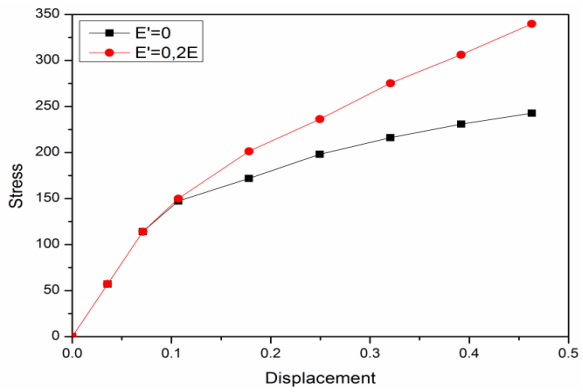

(a) Tresca criteria

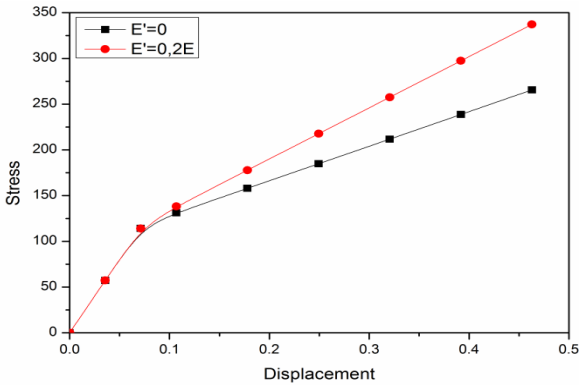

(b) von-Mises criteria.

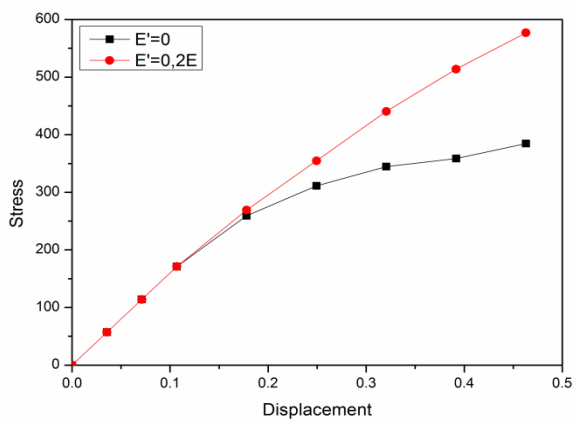

(c) Mohr-Coulomb criteria

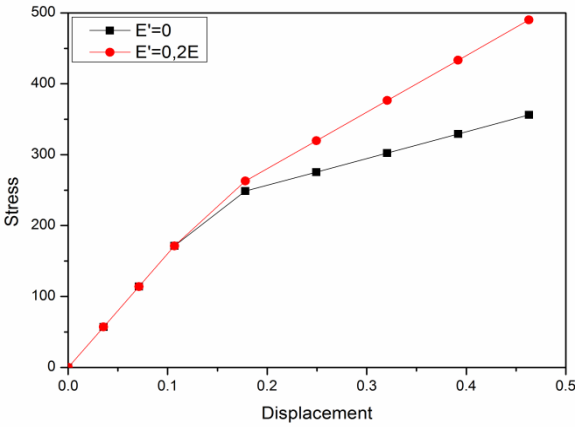

(d) Drucker-Prager criteria.

Fig.7. Stress/displacement curves of the cantilever beam using different values of strain hardening and various yielding criterion

6.3 Mac-Neal's Elongated Cantilever Beam

In the last test, a Mac-Neal's elongated cantilever beam schematically shown in Fig. 3, subjected to a concentrated load shearing at the free edge of the beam is considered. The dimensions of the beam are Length L= 6 and width H = 0.2 and a thickness t is equal to 0.1. The properties of material are Young's modulus E=10^7, Poisson's ratio ν=0.3, yield stress σ_s= 235, and the strain hardening is chosen to be E'=0. This test has been treated as a plane stress problem. The relation between the displacements and the resulting stress is presented in Fig. 8.

On can see from the present figure that, during the loading stage and after surpassing the elastic limit, the material begins yielding and enters into the plastic region. From the Fig. 8 one can see that the stress-displacement curves obtained using Tresca and von-Mises criterion are the same. The same remark is observed for Mohr-coulomb and Drucker-Prager criterion. On the other hand, the Tresca and von-Mises yield criterion enters to the nonlinear phase before the Drucker-Prager and Mohr-coulomb criterion.

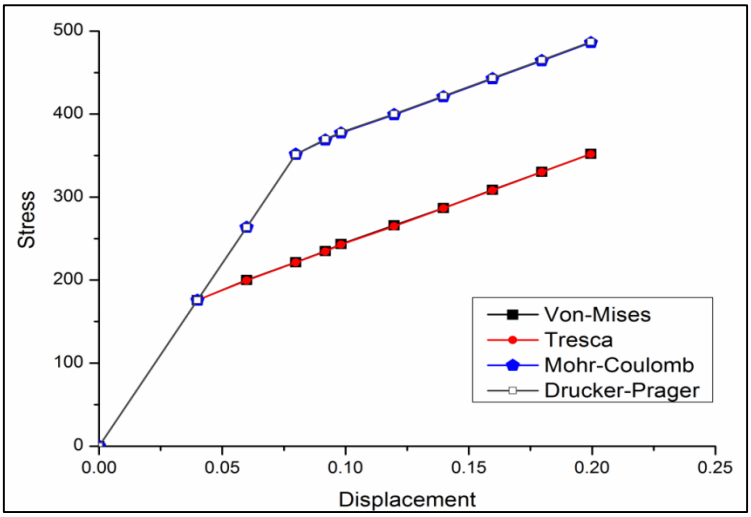

Fig.8 Stress/displacement curves of Mac-Neal's elongated cantilever beam using various yielding criterion

Conclusion

In this work, a finite element based on the strain approach is developed to predict the nonlinear behavior of isotropic materials.

The displacement fields of the present membrane element are the same as adopted by Sabir and it is based on the assumed functions for various components of strain which satisfy the compatibility equation. This element is extended in the present work to predict accurately the elasto-plastic analysis of two-dimensional problems.

In order to analyze the elasto-plastic behavior, several yield criterions are employed such as von-Mises, Tresca, Drucker-Prager and Mohr-Coulomb criteria. The numerical results given by the present element, for both linear and nonlinear analysis are compared to those founded in the literature.

The obtained numerical results using the present element are in well agreement with those from the theoretical solutions; which demonstrates the accuracy and the efficacy of this element. By using the same number of nodes, the numerical solution obtained with the strain-based element has higher precision than those of the element based on classical displacement approach.

The present element SBRIEPE (with four nodes and eight degrees of freedom) gives approximately similar results to those obtained by ANSYS© software and with the robust element Q8 even the latter element has eight nodes and sixteen degrees of freedom. This proves the efficiency of the strain approach used and of course leads to a considerable gain on computing time and data meshing.

On the other hand, according to the obtained results, the strain hardening parameter can increase the stress with the same displacement in the case where the strain hardening is nil. In addition, the Mohr-coulomb and Drucker -Prager yield criterion get to the nonlinear point after the yield criterion of Tresca and von-Mises, and the yield criterion of Tresca, Von-Mises and Mohr-coulomb, Drucker -Prager, respectively, have the same behavior.

Appendix:

The nodal coordinates matrix as given as follow:

$$[C]=\begin{bmatrix} C(x_1,y_1) \\ C(x_2,y_2) \\ C(x_3,y_3) \\ C(x_4,y_4) \end{bmatrix}=\begin{bmatrix} 1 & 0 & -y_1 & x_1 & x_1y_1 & 0 & -y_1^{\,2}/2 & y_1/2 \\ 0 & 1 & x_1 & 0 & -x_1^{\,2}/2 & y_1 & x_1y_1 & x_1/2 \\ 1 & 0 & -y_2 & x_2 & x_2y_2 & 0 & -y_2^{\,2}/2 & y_2/2 \\ 0 & 1 & x_2 & 0 & -x_2^{\,2}/2 & y_2 & x_2y_2 & x_2/2 \\ 1 & 0 & -y_3 & x_3 & x_3y_3 & 0 & -y_3^{\,2}/2 & y_3/2 \\ 0 & 1 & x_3 & 0 & -x_3^{\,2}/2 & y_3 & x_3y_3 & x_3/2 \\ 1 & 0 & -y_4 & x_4 & x_4y_4 & 0 & -y_4^{\,2}/2 & y_4/2 \\ 0 & 1 & x_4 & 0 & -x_4^{\,2}/2 & y_4 & x_4y_4 & x_4/2 \end{bmatrix}$$

The elasticity matrices for plane stress problems:

$$[D]=\frac{E}{(1-\nu)}\begin{bmatrix} 1 & \nu & 0 \\ \nu & 1 & 0 \\ 0 & 0 & \dfrac{1-\nu}{2} \end{bmatrix}$$

The elasticity matrices for plane strain problems:

$$[D]=\frac{E}{(1+\nu)(1-2\nu)}\begin{bmatrix} 1-\nu & \nu & 0 \\ \nu & 1-\nu & 0 \\ 0 & 0 & \dfrac{(1-2\nu)}{2} \end{bmatrix}$$

References

1. Sabir, A. and A.J.T.-w.s. Sfendji, *Triangular and rectangular plane elasticity finite elements.* 1995. **21**(3): p. 225-232.
2. Khechai, A., A. Tati, and A.J.F.o.M.E. Guettala, *Finite element analysis of stress concentrations and failure criteria in composite plates with circular holes.* 2014. **9**: p. 281-294.
3. Hamadi, D., A. Ayoub, and O.J.E.J.o.C.M. Abdelhafid, *A new flat shell finite element for the linear analysis of thin shell structures.* 2015. **24**(6): p. 232-255.
4. Kaveh, A., H.J.C. Rahami, and structures, *Nonlinear analysis and optimal design of structures via force method and genetic algorithm.* 2006. **84**(12): p. 770-778.
5. Hamadi, D., A. Ayoub, and T.J.E.C. Maalem, *A new strain-based finite element for plane elasticity problems.* 2016. **33**(2).

6. Abderrahmani, S., T. Maalem, and D.J.I.J.o.E.R.i.A. Hamadi, *On improved thin plate bending rectangular finite element based on the strain approach.* 2016. **27**: p. 76-86.
7. Khechai, A., et al., *Numerical analysis of stress concentration in isotropic and laminated plates with inclined elliptical holes.* 2019. **100**: p. 511-522.
8. Ashwell, D. and A.J.I.J.o.M.S. Sabir, *Limitations of certain curved finite elements when applied to arches.* 1971. **13**(2): p. 133-139.
9. Ashwell, D. and A.J.I.J.o.M.S. Sabir, *A new cylindrical shell finite element based on simple independent strain functions.* 1972. **14**(3): p. 171-183.
10. Sabir, A. *A new class of finite elements for plane elasticity problems*. in *CAFEM7 7th Int. Conf. Struct. Mech in reactor technology Chicago*. 1983.
11. Sabir, A. *A rectangular and triangular plane elasticity element with drilling degrees of freedom*. in *Proceedings of the Second International Conference on Variational Methods in Engineering, Brebbia CA ed., Southampton University*. 1985.
12. Belarbi, M.T. and A.J.R.e.d.é.f. Charif, *Développement d'un nouvel élément hexaédrique simple basé sur le modèle en déformation pour l'étude des plaques minces et épaisses.* 1999. **8**(2): p. 135-157.
13. Sabir, A. and A.J.I.J.o.M.S. Lock, *Large deflexion, geometrically non-linear finite element analysis of circular arches.* 1973. **15**(1): p. 37-47.
14. Sabir, A. and M.J.T.-w.s. Djoudi, *Shallow shell finite element for the large deflection geometrically nonlinear analysis of shells and plates.* 1995. **21**(3): p. 253-267.
15. Rebiai, C., L.J.A.o.c. Belounar, and m. engineering, *A new strain based rectangular finite element with drilling rotation for linear and nonlinear analysis.* 2013. **13**: p. 72-81.
16. Rebiai, C. and L.J.M. Belounar, *An effective quadrilateral membrane finite element based on the strain approach.* 2014. **50**: p. 263-269.
17. Rebiai, C.J.J.o.M., *Finite element analysis of 2-D structures by new strain based triangular element.* 2019. **35**(3): p. 305-313.
18. Ayadi, A., K. Meftah, and L.J.F.e.I.S. Sedira, *Elastoplastic analysis of plane structures using improved membrane finite element with rotational DOFs: Elastoplastic analysis of plane structures.* 2020. **14**(52): p. 148-162.
19. Lazhar, D., et al., *Solid strain based finite element implemented in ABAQUS for static and dynamic plate analysis.* 2021. **9**(4): p. 449-460.
20. CHICHOUNE, S. and C.J.E.J.f.E.R. REBIAI, *ANALYSIS OF THIN PLATES IN BENDING BY NEW RECTANGULAR STRAIN BASED ELEMENT.* 2023. **28**(3): p. 4.
21. Koh, W.H., et al., *A New Strain-Based Pentagonal Membrane Finite Element for Solid Mechanics Problems.* 2024: p. 100499.
22. Nayak, G. and O. Zienkiewicz, *Elasto-plastic stress analysis. A generalization for various contitutive relations including strain softening.* International Journal for Numerical Methods in Engineering, 1972. **5**(1): p. 113-135.
23. Owen, D.R.J., *Finite elements in plasticity, theory and practice.* 1980.
24. Allman, D., *Evaluation of the constant strain triangle with drilling rotations.* International Journal for Numerical Methods in Engineering, 1988. **26**(12): p. 2645-2655.

25. MacNeal, R.H. and R.L. Harder, *A refined four-noded membrane element with rotational degrees of freedom.* Computers & Structures, 1988. **28**(1): p. 75-84.
26. Cook, R.D., *On the Allman triangle and a related quadrilateral element.* Computers & Structures, 1986. **22**(6): p. 1065-1067.
27. Yunus, S.M., S. Saigal, and R.D. Cook, *On improved hybrid finite elements with rotational degrees of freedom.* International Journal for Numerical Methods in Engineering, 1989. **28**(4): p. 785-800.
28. Timoshenko, S. and J. Goodier, *Theory of Elasticity, 11 McGraw-Hill.* New York, 1951.
29. Taylor, R., et al., *The patch test—a condition for assessing FEM convergence.* International Journal for Numerical Methods in Engineering, 1986. **22**(1): p. 39-62.
30. Peng, M., D. Li, and Y. Cheng, *The complex variable element-free Galerkin (CVEFG) method for elasto-plasticity problems.* Engineering Structures, 2011. **33**(1): p. 127-135.